ResearchGate

See discussions, stats, and author profiles for this publication at: https://www.researchgate.net/publication/279295040

DETER-B: The New Amazon Near Real-Time Deforestation Detection System

Article *in* IEEE Journal of Selected Topics in Applied Earth Observations and Remote Sensing · July 2015

DOI: 10.1109/JSTARS.2015.2437075

CITATIONS
31

READS
393

12 authors, including:

Cesar Diniz
Federal University of Pará
7 PUBLICATIONS **127** CITATIONS
SEE PROFILE

Diogo Correa Santos
VALE
9 PUBLICATIONS **35** CITATIONS
SEE PROFILE

Nelton Cavalcante da Luz
A Fundação de Ciência, Aplicações e Tecnologia Espaciais
8 PUBLICATIONS **31** CITATIONS
SEE PROFILE

Alessandra Rodrigues Gomes
National Institute for Space Research, Brazil
41 PUBLICATIONS **159** CITATIONS
SEE PROFILE

Some of the authors of this publication are also working on these related projects:

Project
AVALIAÇÃO DO PROCESSO DE COBERTURA DA TERRA NO ENTORNO DE USINAS HIDRELÉTRICAS NA AMAZÔNIA BRASILEIRA: A EVOLUÇÃO DA UHE DE TUCURUÍ View project

Project
Projeto de Monitoramento Ambiental por Satélite no Bioma Amazônia- TerraClass View project

All content following this page was uploaded by Cesar Diniz on 18 August 2015.

The user has requested enhancement of the downloaded file.

DETER-B: The New Amazon Near Real-Time Deforestation Detection System

Cesar Guerreiro Diniz, Arleson Antonio de Almeida Souza, Diogo Corrêa Santos, Mirian Correa Dias, Nelton Cavalcante da Luz, Douglas Rafael Vidal de Moraes, Janaina Sant'Ana Maia, Alessandra Rodrigues Gomes, Igor da Silva Narvaes, Dalton M. Valeriano, Luis Eduardo Pinheiro Maurano, and Marcos Adami

***Abstract*—The Brazilian Legal Amazon (BLA), the largest global rainforest on earth, contains nearly 30% of the rainforest on earth. Given the regional complexity and dynamics, there are large government investments focused on controlling and preventing deforestation. The National Institute for Space Research (INPE) is currently developing five complementary BLA monitoring systems, among which the near real-time deforestation detection system (DETER) excels. DETER employs MODIS 250 m imagery and almost daily revisit, enabling an early warning system to support surveillance and control of deforestation. The aim of this paper is to present the methodology and results of the DETER based on AWIFS data, called DETER-B. Supported by 56 m images, the new system is effective in detecting deforestation smaller than 25 ha, concentrating 80% of its total detections and 45% of the total mapped area in this range. It also presents higher detection capability in identifying areas between 25 and 100 ha. The area estimation per municipality is statistically equal to those of the official deforestation data (PRODES) and allows the identification of degradation and logging patterns not observed with the traditional DETER system.**

***Index Terms*—Monitoring, public policies, rainforest, remote sensing.**

I. Introduction

In 1990, it was estimated that rainforests cover between 11.5 and 12.4 million km^2 worldwide and their annual deforestation rate from 1990 to 1997 was estimated at 60 000 km^2 [1]. From 2000 to 2012, it was estimated that 32% of the global forest loss occurred in tropical forests and, almost half of the tropical forest was lost in South America [2]. The so-called Brazilian Legal Amazon (BLA) has approximately 5 million km^2, from which $\sim$3.2 million km^2 are rainforest, about 30% of the global extent, being the largest continuous rainforest with the highest biodiversity of several forest-dependent species [3], [4]. The BLA is biogeographically heterogeneous and, anthropogenic impact has resulted in a huge variety of deforestation patterns associated with different actors and land use and land cover histories [3], [5] and its deforestation is a major environmental problem [3].

Given the region complexity and dynamics, there are large government investments focused on the control and prevention of deforestation. The National Institute for Space Research (INPE) is currently developing five complementary systems for BLA forest monitoring: 1) the Amazon Deforestation Monitoring Project (PRODES); 2) the Selective Logging Detection Project (DETEX); 3) the Brazilian Amazon Forest Degradation Project (DEGRAD); 4) the near real-time deforestation detection (DETER) [6]; and 5) the land use and land cover mapping of Amazon Deforested Areas (TerraClass) [7].

The PRODES system, created in 1988, is designed to provide annual rates of gross deforestation in BLA providing detailed information on deforestation dynamics [6], [8]. Despite PRODES importance for forest monitoring and the establishment of public policies, the time required for the production of such data precludes the rapid identification of areas in initial or intermediate stages of degradation, making it difficult to setup preventive and supervisory actions to slow down or reverse deforestation processes.

In 2004, the annual rate of deforestation in the Amazon reached its climax, with a forest loss of over 27 000 km^2. As a response to increasing rates of deforestation, the federal government established the Federal Action Plan for Prevention and Control of Deforestation in the Amazon (PPCDAM), aiming to promote the reduction of deforestation through a set of integrated actions of land tenure regularization, environmental monitoring and control, and promotion of sustainable productive activities, involving partnerships among federal agencies, state governments, municipalities, civil society organizations, and the private sector [9], [10].

To comply with PPCDAM demand, INPE created DETER system, exploiting the high temporal resolution of nearly daily coverage of MODIS 250 m data and an almost daily resolution. DETER is designed as an early warning system to support surveillance and control of deforestation, mapping the occurrence of clear cutting and forest degradation areas greater than 25 ha. These data are sent to the Brazilian Institute of Environment and Renewable Natural Resources (IBAMA), which is responsible for deforestation surveillance [6], [11].

In the last decade, PRODES analyses have indicated a reduction in the average size of clear-cut areas [12]. This reduction is a major limitation for MODIS-based deforestation mapping, since it is not possible to detect areas smaller than 25 ha and it has a poor precision, detecting only areas between 25 and 100

Manuscript received September 30, 2014; revised January 30, 2015; accepted May 18, 2015. Date of publication June 18, 2015; date of current version August 11, 2015. This work was supported by the Regional Center of the Amazon—CRA, from the National Institute for Space Research—INPE.

The authors are with the National Institute for Space Research—INPE, Parque de Ciencia de Tecnologia do Guama, Belem 66077-830, Brazil (e-mail: cesar.diniz@inpe.br; arlesson.souza@inpe.br; diogo.santos@inpe.br; mirian.dias@inpe.br; nelton.luz@inpe.br; douglas.moraes@inpe.br; janaina.maia@inpe.br; alessandra.gomes@inpe.br; igor.narvaes@inpe.br; dalton@inpe.br; dalton@dsr.inpe.br; maurano@inpe.br; maurano@dpi.inpe.br; marcos.adami@inpe.br).

Color versions of one or more of the figures in this paper are available online at http://ieeexplore.ieee.org.

Digital Object Identifier 10.1109/JSTARS.2015.2437075

1939-1404 © 2015 IEEE. Translations and content mining are permitted for academic research only. Personal use is also permitted, but republication/redistribution requires IEEE permission. See http://www.ieee.org/publications_standards/publications/rights/index.html for more information.

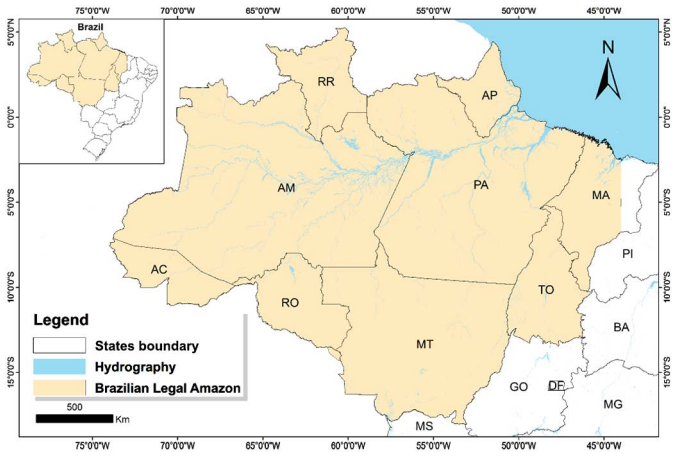

Fig. 1. Study site location. The so-called BLA.

ha [13]. To adapt to the changes in the deforestation process, the Amazon Regional Center of INPE (INPE-CRA) has begun an experimental deforestation mapping activity using AWFIS sensor imagery at $56\ \mathrm{m}^2$ and 5 days of temporal resolution. The goal of the experiment is to expand the capacity of moderate resolution data analysis and increases the detection capability of deforestation in the early stages of the degradation process. Thus, this paper presents the methodology and results of the DETER based on AWIFS data, called DETER-B.

II. Methods

A. Study Site

The work area of the proposed method comprises the BLA, which is defined by Federal Law No. 1806/53, art. second and No. 5173/66, art. second as the totality of Acre (AC), Para (PA), Amazonas (AM), Roraima (RR), Rondonia (RO), Amapa (AP), and Mato Grosso (MT), as well as the regions west of the meridian of 44° W, the state of Maranhao (MA) (Fig. 1).

B. Material

The following data were used to build this system:

1) 291 AWiFS images, from March 29 to September 4 of 2013;
2) Landsat Orthorectified Data (Global Land Survey—GLS) [14], [15];
3) BLA official boundary;
4) PRODES data until 2013 [6].

C. Mapping Method

The method (Fig. 2) used in Deter-B system is based on visual interpretation and consists of the following steps: 1) image acquisition and composition; 2) geometric correction; 3) linear spectral mixture model; 4) retrieving not observed areas; 5) PRODES mask generation; 6) visual interpretation; and 7) audit.

Image acquisition occurs through digital catalog, maintained by INPE, which is free of charge to any user. The provided AWIFS images are divided in four quadrants, with the following organization: 1) A (northwest); 2) B (northeast); 3) C (SW); and 4) D (southeast). Bands 5, 4, and 3, corresponding to mid-infrared ($155-170\ \mu\mathrm{m}$), near-infrared (0.77–$0.86\ \mu\mathrm{m}$), and red (0.62–$0.68\ \mu\mathrm{m}$), were used in the process, respectively. A visual analysis of the scene is conducted to assess the quality of the image, selecting images that are not overly contaminated with cloud cover.

The selected images are inserted into a PostGIS database v1.5 through v4.4.3 TerraAmazon software, based on TerraLib library [16]. TerraAmazon was developed to systematize satellite BLA monitoring and, in addition, to offer digital image processing, editing and query capabilities, characteristics that are proper of a Geographic Information System. This system allows consistent algorithms and topological structure to be created, so that generation of spurious polygons is prevented [16].

The AWiFS images were georeferenced using GLS [14], [15] as reference data. Geometrical correction is based on triangulation by a "nearest neighbor" resampling algorithm and second degree polynomial. The tolerated root-mean-square error (RMSE) is less than or equal to 0.65, which represents, having AWIFS pixel as reference, approximately 33.8 m. Prior to georeferencing, a visual analysis of dense cloud distribution (e.g., Cumulus) is performed. If a portion of the image is covered by dense cloud formations, this area is excluded from the image. This approach makes the posterior georeferencing process easier.

After georeferencing, the linear spectral mixing model (LSMM) is applied [17] to estimate the fraction of the soil, vegetation, and shade components present in each image pixel. The spectral mixing model can be written as

$$d_i = \sum_{j=1}^{r} s_{ij} a_j + e_i \tag{1}$$

where d_i is the value for the ith band, a_j is the fractional area or proportion covered by the jth component, s_{ij} is the ith component of the vector for the jth mixture component (the vector is often the reflectance of the mixture components, i.e., the component signatures), and e_i is the error term for the ith band. The matrix of end member reflectance s_{ij} is typically assembled using reflectance field measurements [18] or by identifying samples of pure pixels in the scene for each cover type [19]. In this case, the end member selection was performed by identifying samples of pure pixels, in each image. The constrained unmixing solution for a_j is determined by

$$\sum_{j=1}^{r} a_j = 1 \text{ and } a_j \geq 0 \text{ for all components.} \tag{2}$$

The above-mentioned constraint equations are strictly true only if the chosen components and their spectral signatures are an adequate representation of the mixture occurring within the pixel under analysis. Following [17], we determined the αj by using constrained least squares and weighted least square methods. This method avoids anomalous values, guaranteeing nonnegative and added to 1 value only.

The soil fraction highlights selective logging features, as log decks, skid trails, and roads. On areas of reduced-impact

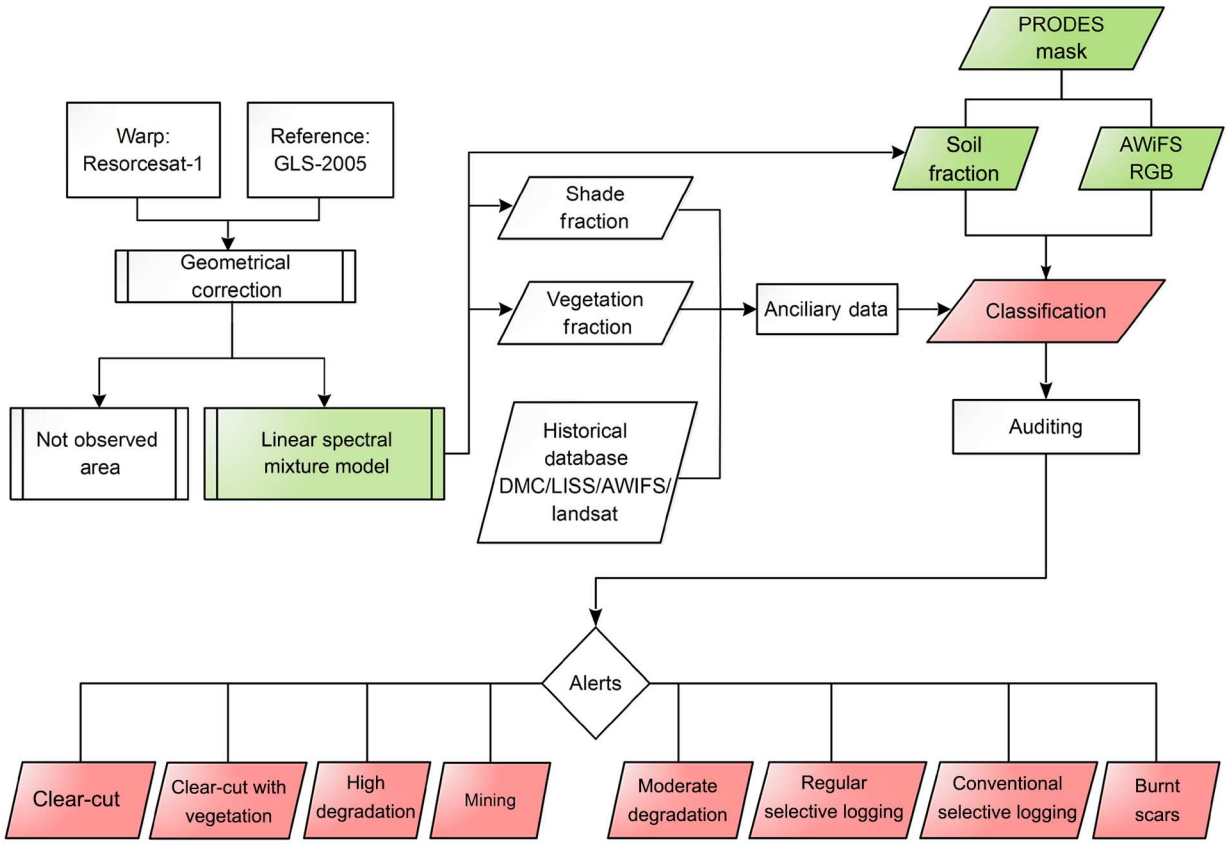

Fig. 2. DETER-B mapping method.

logging [20], the features may only be detected over the soil fraction. Similarly, the shade fractions are used to enhance burnt scar features [21].

The unobservable part of the image, or Not Observed Area, is a bimonthly product generated by geometric operations of aggregation and difference, involving cloud and shade vectors obtained by a cloud detection algorithm [22], the vector boundary of each image, and the BLA vector.

Another essential component of this analysis is referred to as PRODES mask, which includes all historical clear-cut deforestation since 1988, alongside the areas represented by nonforest and hydrography [6], [23]. PRODES mask is used to prevent a mistaken repetition of previous deforestation data, avoiding the generation of false deforestation alerts. This mask is considered base map for each mapping year.

Sequentially, visual interpretation starts, supported by soil fraction, AWIFS false color composites 5(R), 4(G), and 3(B), shade and vegetation fractions and extensive Landsat, LISS and DMC time series. DETER-B data are used by environmental law enforcement agencies, in PPCDAm context, to guide aerial and terrestrial displacement of federal agents. In this sense, commission errors may represent underutilization of deforestation combat structure, decreasing the efficiency of surveillance campaigns.

The following classes were defined: 1) clear-cut deforestation; 2) deforestation with vegetation; 3) mining; 4) moderate degradation; 5) intense degradation; 6) burnt scar; 7) regular selective logging; and 8) conventional selective logging. Clear-cut or mining are delineated in yellow, degradations or logging are in blue, PRODES mask (previous deforestation, nonforest and hydrography) are in solid red, the remaining image represents forest. These patterns (yellow or blue) are interpreted based on four main elements: 1) color; 2) tone; 3) texture; and 4) context (Table I). It is important to highlight that Landsat, LISS, and DMC series analyses are always coupled with visual interpretation.

Forest degradation is considered by Gerwing and Vidal [24] as an incremental process, especially in the eastern part of the Amazon, where impacts of relatively low intensity determine the stage for other deeper disturbances. Given this, partial and continuous loss of forest cover may occur, with the consequent increase in the proportion of exposed soil.

Therefore, the transition between the early stages of degradation and clear-cutting can be fairly rapid. Thus, in a DETER, the initial and final stages of forest degradation shall present different mapping strategies. Moreover, the system must be capable of differentiating natural from anthropic disturbance. Natural disturbances tend to present nonlinear shape and are not necessarily associated to any infrastructure [25].

Similarly, seasonal patterns such as natural flooded areas, deciduous, and semideciduous vegetation are also solved by the use of temporal data series.

On DETER-B system, moderate and intense degradations, burnt scar, and regular and conventional selective logging are mapped every month. The clear-cut deforestation, deforestation with vegetation, and mining classes are permanent throughout

TABLE I
FOREST DEGRADATION PATTERN AND MAIN CLASSIFICATION ELEMENTS: COLOR, TONE, TEXTURE, AND CONTEXT

CLASSES	Color composition	Color composition 5R4G3B interpretation key	Soil fraction	Soil fraction interpretation key
Clearcut deforestation	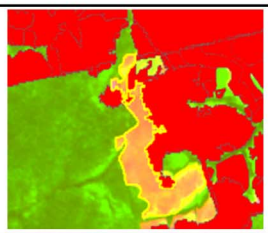	**Color**: magenta **Tonality**: high **Shape**: regular **Texture**: smooth **Context**: well-defined boundaries between feature (bare soil) and the forest matrix.	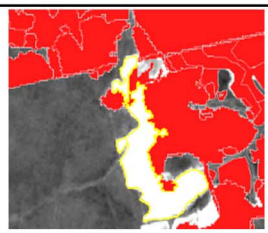	**Color**: gray/white **Tonality**: high **Shape**: regular **Texture**: smooth **Context**: well-defined boundaries between feature (bare soil) and the forest matrix.
Deforestation with vegetation	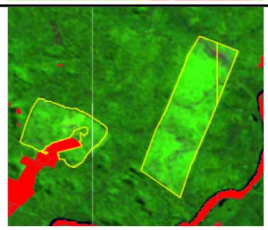	**Color**: green **Tonality**: high **Shape**: regular **Texture**: smooth **Context**: well-defined boundaries between feature (light green) and the forest matrix. Remarkable growth of secondary vegetation.	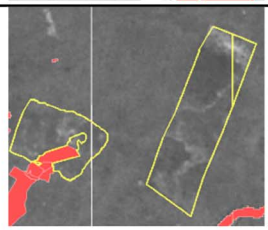	**Color**: black **Tonality**: low **Shape**: regular **Texture**: smooth **Context**: poorly defined boundaries between feature and surrounding area, both color and tonality are similar. These features are classified according to its Color Composition and Vegetation Fraction characteristics.
Mining	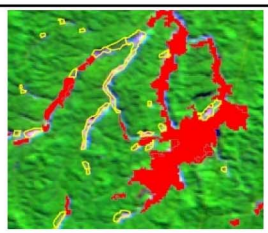	**Color**: magenta or blue **Tonality**: high **Shape**: irregular **Texture**: rough **Context**: its boundaries are usually associated to river channels.	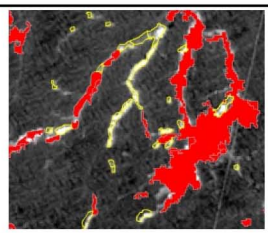	**Color**: gray/white **Tonality**: high **Shape**: irregular **Texture**: rough **Context**: its boundaries are usually associated to river channels.
Moderate degradation	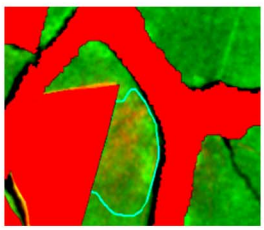	**Color**: green or magenta **Tonality**: medium **Shape**: irregular **Texture**: rough **Context**: green and magenta tones mixed but predominance of green, related to the presence of forest patches (bare soil) and secondary vegetation.	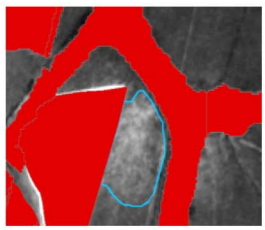	**Color**: gray **Tonality**: high **Shape**: irregular **Texture**: rough **Context**: dark gray tonality indicating predominance of forest cover associated with light gray spots (bare soil).
Intense degradation	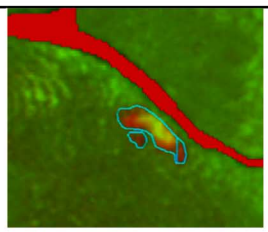	**Color**: green or magenta **Tonality**: high **Shape**: irregular **Texture**: rough **Context**: green and magenta tones are mixed but predominantly magenta, related to the presence of gaps, bare soil and secondary vegetation.	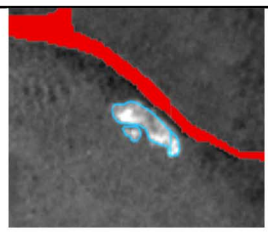	**Color**: gray/white **Tonality**: high **Shape**: irregular **Texture**: rough **Context**: predominance of light gray tones associated with the presence of clearings, secondary vegetation and bare soil.
Burnt scar	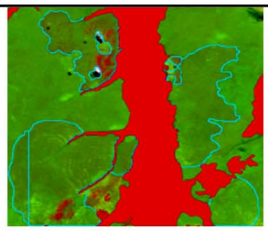	**Color**: magenta or green **Tonality**: medium **Shap**: irregular**e** **Texture**: rough **Context**: predominance of light gray tones associated with the presence of clearings, secondary vegetation and bare soil.	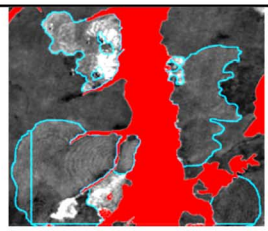	**Color**: gray **Tonality**: medium/high **Shape**: irregular **Texture**: rough **Context**: predominance of gray tonality lighter than the forest matrix, with rough texture. This feature may present circular concentric patterns also lighter than the forest matrix.

TABLE I
(*Continued.*)

Regular selective logging		**color**: green **tonality**: low **shape**: regular **texture**: rough **context**: predominance of green tonality and forest pattern, presence of small circular magenta features (points), with well-defined geometric distribution.	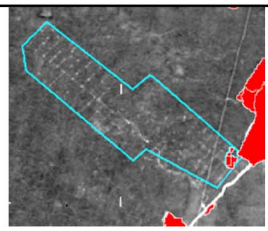	**color**: gray/white **tonality**: high **shape**: regular **texture**: rough **context**: predominance of dark gray tonality with presence of small white (lighter) and circular features, with well-defined geometric distribution.
Conventional selective logging	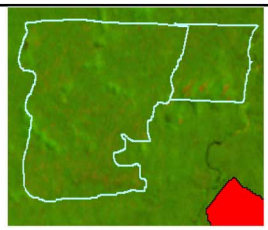	**color**: green **tonality**: low **shape**: irregular **texture**: rough **context**: predominance of dark green tonality with minimal presence of light green and / or magenta tones	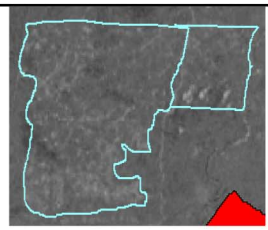	**color**: gray/white **tonality**: high **shape**: irregular **texture**: rough **context**: predominance of dark gray tonality with presence of light gray dots, irregularly distributed, probably associated with lack of management plan.

PRODES mask | Clear-cut or mining delineation | Degradations or logging delineation

the year, once mapped it remains unchanged, being delineated only by possible increments.

After visual interpretation, DETER-B data undergo a review process, in which auditors confer identification and limits, and if necessary, the data is reinterpreted. After internal audit, the alert vectors are sent to IBAMA, the Federal Institute responsible for the surveillance and control of deforestation in the Amazon.

D. DETER-B and PRODES Data Evaluation

To compare DETER-B results with PRODES data, the data must be standardized, once different monitoring systems may have different goals, operate with different sensors, methodologies, and geographical area. In the case of the DETER-B 2013 and PRODES 2013, AWIFS and OLI-8 are the, respectively, used sensors. These sensors were compared by Goward *et al*. [26].

Temporal PRODES 2013 data refer to the period of July–September, while DETER-B data vary temporally from March to September. Besides the distinct time period used for mapping, the data availability also differs, which may influence the detection capacity of each system and in some cases, preclude the evaluation of given area of earth's surface at the same time period. These difficulties are aggravated by IRS1 coverage limitation, near the end of its useful lifetime. IRS1 coverage was reduced to 8 min per day. Thus, a common mapping area was generated (Fig. 3) to make both data sets comparable.

Spatial adequacies were carried out in such a way that only the regions that are simultaneously cloud and shadow free are considered common area and have been observed by both systems at least once a year. For analysis purposes, only similar classes in each project were compared.

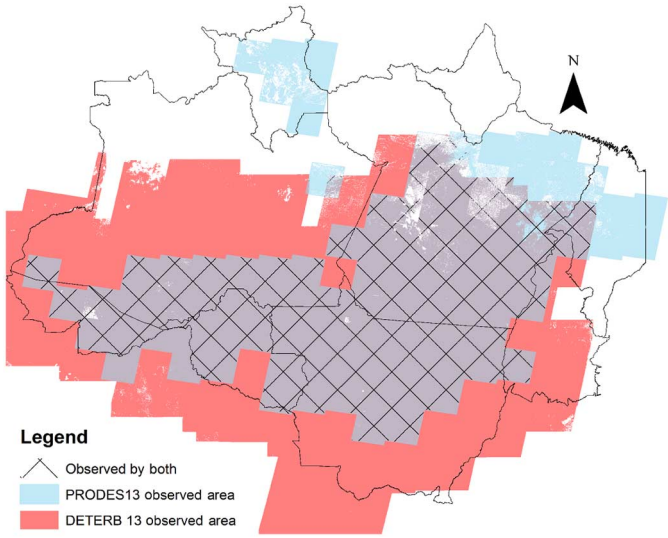

Fig. 3. DETER-B and PRODES common mapping area.

All classes that share clear-cutting characteristics were considered comparable. Accordingly, clear-cut and residues classes of PRODES system are considered comparable with DETER-B system classes of clear-cut deforestation, deforestation with vegetation, and mining (Table II). All other classes were excluded from comparative analyzes.

III. Results

A. General Results

To understand the system warning capability, the occurrence of deforestation and its relationship with ground truth, it is necessary to understand the nature of deforestation in the Amazon rainforest. The deforestation of primary forest can go

TABLE II
COMPARED CLASSES OF DETER-B AND PRODES

Thematic classes — PRODES and DETER-B	
PRODES	DETER-B
Clear-cut	**Clearcut deforestation**
Residues	**Deforestation with vegetation**
	mining

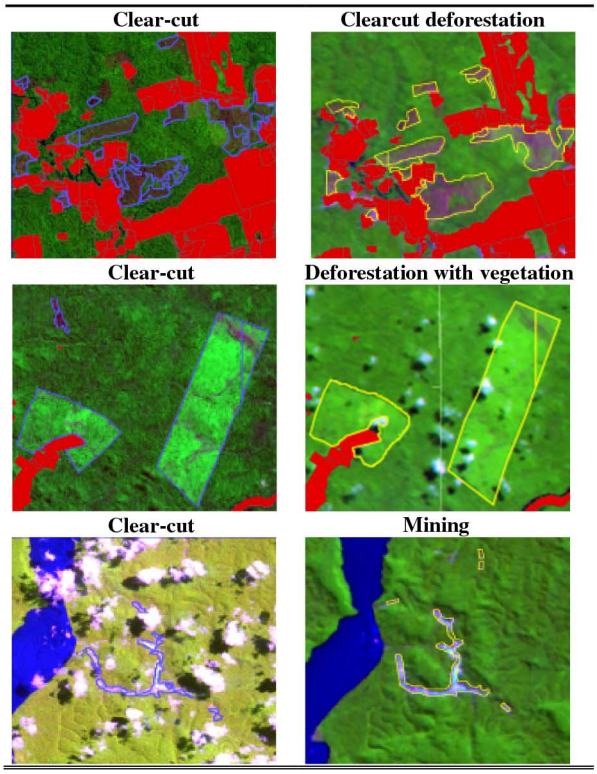

through different levels of degradation and, largely depending on the conditions of socioeconomic boundary, the deforestation process can take several years or just a few days [27]–[34]. Thus, the dynamics of the degradation process calls for different detection strategies. These strategies are associated, in large part, to the dynamics of each degradation level and the central objective of the system, which in this case is rapid detection of forest disturbance to avoid full conversion to clear-cut deforestation.

Frequency of observation plays a key role on the degradation dynamics assessment and rapid disturbance detection. High observation frequency is critical to near real-time systems, as the frequency of observation is important for reliable detection of selective logging and other events that may manifest themselves only ephemerally in satellite images. Here, a total of 291 AWiFS images were used. Fig. 4 shows DETER-B observations frequency from March 29 to September 4, 2013. It is worth noting that the areas of higher observation frequency (in red) circumscribe most of the "deforestation arch." Furthermore, the system observation frequency has huge improvement capacity, once Landsat 8 and AWiFS 2 data are being freely distributed by NASA and INPE, respectively.

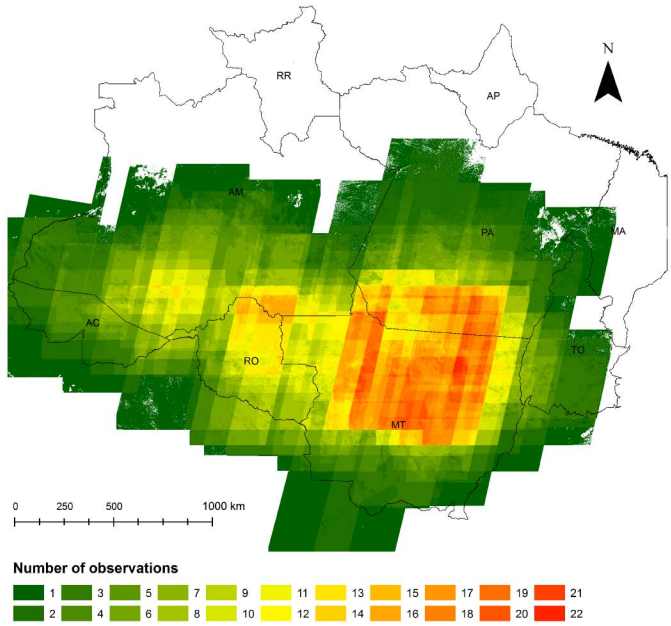

Fig. 4. Number of observation per area. The monitoring repeat time varies from one single image to 22 observations from March 29 to September 4, 2013.

TABLE III
DEGRADATION CLASSES MONTHLY AREA, PRODES MASK AREA, AND OBSERVED AREA, BETWEEN PARENTHESES THE DEGRADATION PERCENTAGE PER FOREST AVAILABILITY (%DFA) IN km^2

	July	August	September
PRODES mask	744 934.02	582 685.22	56 607.19
Observed areas	2 470 540.82	2 138 229.22	658 058.58
Moderate degradation	639.28 (0.04%)	1177.27 (0.08%)	146.33 (0.02%)
Intense degradation	1942.82 (0.11%)	1859.16 (0.12%)	236.91 (0.04%)
Burnt scars	7111.16 (0.41%)	6706.83 (0.43%)	0.13 (–)
Regular selective logging	2154.76 (0.12%)	2890.46 (0.19%)	31.19 (0.01%)
Conventional selective logging	1429.24 (0.08%)	2011.93 (0.13%)	235.30 (0.04%)
Disturbance per forest area	13 277.27 (0.77%)	14 645.65 (0.94%)	649.86 (0.11%)

DETER-B produced an alert when any forest degradation is identified in an image, provided that it has not been previously detected by PRODES, thus establishing a complimentary deforestation program. The initial levels of degradation and logging, with higher dynamics in the deforestation evolution, are independent and analyzed every month. Consolidated levels such as clear-cut deforestation, deforestation with vegetation, and mining, are permanent and, once mapped, will remain in the same class. Table III discriminates, in square kilometers, the monthly area of the higher dynamics classes, PRODES

mask, observed area, and the degradation percentage per forest availability (%DFA, are shown in parentheses). Since it is not possible to obtain homogeneous availability of images per month, the %DFA ponders the monthly degradation by forest area available. This analysis considers that, available forest area $= (\text{observed area}) - (\text{PRODES mask})$, while $(\%\text{DFA}) =$ monthly degradation/available forest area. Asner *et al.* [20] estimated selective logging areas to be ranging from 12 075 to 19 823 km^2 per year for the entire Brazilian Amazon. These differences in logging area between both studies may be associated to temporal and geographical distinctions of each one.

Despite the lower %DFA, the monthly degradation identifies, in near real-time, possible forest disturbance innumerable by any other current monitoring system. In August 2013, 14 600 km^2 of forest disturbance was identified using PRODES and DETER-B parsimoniously.

In the Amazon, natural or accidentally caused fires are rare, and are typically a result of anthropogenic land use change [35] in the Amazon [30], [36]. Furthermore, the effect of fire on the subcanopy can substantially alter the regeneration processes, and therefore the vegetation succession [37]. Forest degradation is frequently associated with fires, where degraded and intensely burned areas provide less forest cover and consequently greater exposure of the soil, as well as the loss of biodiversity [38]–[40], and ultimately produce a burnt scar in the forest. In this study, this type of degradation associated with fire is considered forest remnants found to be the most predominant type of disturbance for the months of July and August (7111.16 and 6706.83 km^2, respectively).

Among the mapped classes, the selective logging classes are the most complex disturbances to identify and evaluate. For these classes, it is worth noting the tendency to overestimate the area. However, there is a distinct difference in the disturbance intensity when comparing regular selective logging, whose characteristics indicate the existence of a management plan, and the conventional selective logging. For regular selective logging, associated with regular distribution of stockyards, the disturbance in forest interior is lower, once it follows a management plan, and is concentrated on major, secondary pathways, and stockyards. In conventional selective logging, disturbance is higher, as major and secondary pathways lack of planning, stock yards and terraces are not regularly distributed and dimensioned. Lack of management techniques prior to timber extraction, among others, is a major cause of forest degradation [41].

Selective logging is presented in the form of circular/rectangular area, presenting features of small size, with well-defined geometric patterns, or not in the case of conventional logging extraction, associated with a set of pathways. However, as stated in this alert system, the mapping of selective logging is made by the generalization of the modified area, with the inclusion of forest as a constituent of the classes of regular and conventional selective logging. Thus, the calculated selective logging area must not be directly compared with any other class, as the boundaries of these classes are not easily distinguishable. However, recognizing selective logging areas is of great importance to a deforestation control system, since these areas are likely to be converted into clear-cut areas [20].

TABLE IV
CLEAR-CUTS SUM BY CLASS AND STATES

Class	Area (km^2)
Clearcut deforestation	4131.31
Deforestation with vegetation	1522.96
Mining	102.82
State	Area (km^2)
Acre	693.58
Amazonas	914.74
Maranhao	2.36
Mato Grosso	1429.80
Para	1813.35
Rondonia	872.35
Tocantins	30.90
TOTAL	5757.08

TABLE V
CLEAR-CUTS AND MINING GROUPED BY DIFFERENT SIZE RANGES

DETER-B				
Size range (ha)	Area (ha)	Polygons	% Pol	% Area
<25	310 945.50	57 497	93.89	54.01
>=25 ; <50	82 660.14	2422	3.95	14.36
>=50 ; <100	57 993.47	841	1.37	10.07
>=100	124 109.36	480	0.78	21.56
Total	575 708.48	61 240	100	100

The final levels of degradation are those that shares clear-cut characteristics, having most of its detected area composed of bare soil exposure, cases of clear-cut deforestation, and deforestation with vegetation and mining.

Overall, approximately $5757.00\,\text{km}^2$ were identified as belonging to the last stages of forest degradation. The clear-cut deforestation and deforestation with vegetation classes represent 72% and 21% of clear-cut area, respectively, whereas mining class represents about 2% of these detections (Table IV).

Diniz *et al.* [42] and Santos *et al.* [43] confirm the capability of the AWIFS sensor to detect areas smaller than 25 ha, one of the major limitations of MODIS sensor. These results demonstrate that while the high temporal resolution is of primary importance for near real-time systems implementation, the ability to differentiate deforestation patterns rises with the increase in spatial resolution. Table V shows clear-cuts and mining grouped by different hectares size ranges.

Clear-cuts and mining results coincide with the expected reduction in average size of the deforestation patches [12], with approximately 94% of its total detections in the range <25 ha. Thus, this improvement in spatial resolution from the implementation of DETER-B achieves the desired monitoring

TABLE VI
DETER-B (CLEAR-CUT DEFORESTATION, DEFORESTATION WITH VEGETATION AND MINING CLASSES) AND PRODES (CLEAR-CUT AND RESIDUES CLASSES) MAPPED AREAS BY STATE AND DETER/PRODES RATIO

State	PRODES (ha)	DETER (ha)	Ratio DETER/PRODES
Acre	15 628.69	30 611.19	1.96
Amazonas	35 094.06	41 980.35	1.20
Maranhao	7978.80	217.51	0.03
Mato Grosso	106 661.60	126 741.16	1.19
Para	178 293.70	137 223.07	0.77
Rondonia	86 914.33	67 585.25	0.78
Tocantins	2717.95	540.34	0.20

capability of PPCDAm and IBAMA in the surveillance and combat of deforestation in the Amazon.

B. Statistical Analyses

To verify the DETER-B statistical validity, its change classification was compared to PRODES system. The statistical evaluation was conducted on change greater than 6.25 ha and considers only classes that share clear-cut characteristics. Accordingly, clear-cut and residues classes of PRODES are compared with DETER-B clear-cut deforestation, deforestation with vegetation, and mining classes. Considering the methodological, spatial and temporal systems differences, there is a reasonable relationship between the areas mapped by DETER-B and PRODES. However, there is a considerable difference in the values presented by AC and AM states. Table VI shows the DETER-B and PRODES mapped areas by state and the ratio between them.

The states of RO, PA, MT, and AM had area differences in the order 15%–20%, approximately for each system. This difference is considered reasonable taking into consideration the methodological, spatial and temporal differences of each system and the sensors involved (AWIFS and Landsat 8). Since this work is based on an ideal scenario, we suggest comparing PRODES and DETER-B more thoroughly in AC and Tocantins states, to properly understand the discrepant values identified by each system, ratio of DETER/PRODES is 1.96 and 0.20, respectively. The observed discrepancy for the state of MA is most likely due to temporal differences between PRODES and DETER-B observation date. In relation to Landsat data used in PRODES (July 4, July 11, and August 5), the AWiFS sensor has recorded an early (June 6) and single acquisition of the area (Fig. 4). To assess the PRODES/DETER correlation in more detail, Fig. 5 presents area dispersion per municipality for each system, a total of 188 municipalities were evaluated. The determination coefficient $(R^2) = 0.83$ indicates a strong linear correlation for area values by municipality. Regression analysis indicates a high probability of the estimated values for both systems to be equal, since the intercept can be equal to 0 and the linear slope may be equal to 1 when the tested confidence interval is at 95% probability.

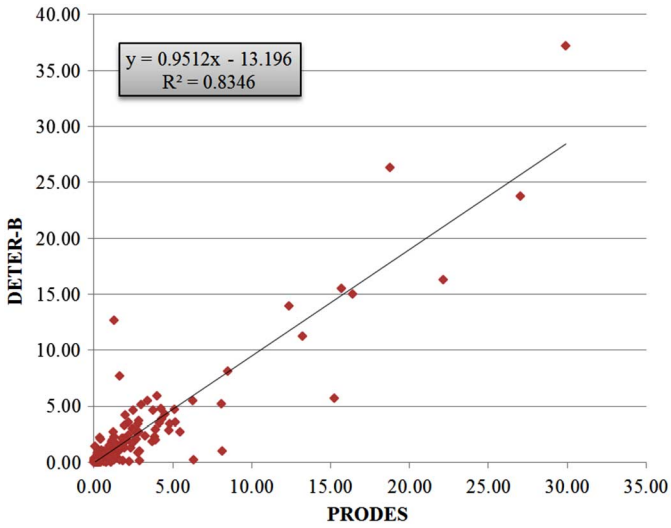

Fig. 5. Area dispersion per municipality to each system in 1000 ha.

TABLE VII
DETER-B AND PRODES DATA GROUPED IN DIFFERENT SIZE RANGES

DETER-B 2013 Size ranges (ha)	Area (ha)	Number of polygons	% Pol	% Area
<25	191 508.64	17 113	82.48	42.82
>=25 ; <50	79 861.67	2338	11.27	17.86
>=50 ; <100	57 155.99	829	4.00	12.78
>=100	118 673.27	468	2.26	26.54
Total	447 199.57	20 748.00	100	100
PRODES 2013 Size ranges (ha)	Area (ha)	Number of polygons	% Pol	% Area
<25	203 931.88	18 337	84.37	47.39
>=25 ; <50	75 955.32	2245	10.33	17.65
>=50 ; <100	50 832.12	746	3.43	11.81
>=100	99 607.91	407	1.87	23.15
Total	430 327.23	21 735	100	100

PRODES historical series indicates a reduction in the average size of deforestation [12], [13]. In this sense, DETER-B system based on 56 m sensor overrides this limitation, as seen in Table VII, which compares DETER-B and PRODES data grouping it in different size ranges.

DETER-B and PRODES 2013 data showed to be statistically similar when grouped by size range, for all ranges used. Both systems corroborate with the expected reduction in the area of deforestation polygons [12], presenting approximately 80% of its total detections in the range <25 ha, this range concentrates nearly 45% of the area mapped by each system.

The same statistical approach was used to standardize and analyze traditional MODIS-based DETER. In Table VIII, DETER data are grouped into the same size ranges, as previously used in PRODES/DETER-B comparison.

TABLE VIII
MODIS-BASED DETER DATA GROUPED IN DIFFERENT SIZE RANGES

DETER-MODIS 2013				
Size ranges (ha)	**Area (ha)**	**Number of polygons**	**% Pol**	**% Area**
<25	123.43	8	0.31	0.05
>=25 ; <50	41 833.14	1109	43.56	18.19
>=50 ; <100	65 465.75	952	37.39	28.47
>=100	122 498.00	477	18.74	53.28
Total	229 920.32	2546	100	100

As expected, DETER-B and DETER-MODIS show huge data disagreement, this is especially true for the range <50 ha. Remarkably, in the range <25 ha, DETER-MODIS detected only eight deforestation polygons, 0.05% of the total deforested area, which represents around 120 ha. Meanwhile, the same range concentrates 82% of DETER-B deforestation detections, accounting more than 17 000 alerts, which represents an area of $\sim$191 000.00. This analysis has confirmed DETER-B ability to detect smaller polygons and has increased its effectiveness in identifying forest disturbance within areas ranging between 25 and 100 ha, two of the main goals of this new proposed system.

IV. CONCLUSION

The new near real-time detection system, so-called DETER-B has higher detection capability than its predecessor MODIS-based DETER, being able to identify a wider range of forest intervention, increasing the ability to detect the different stages involved in the degradation and selective logging process, underlain to elaboration of more efficient public policies to combat and control deforestation in the BLA.

ACKNOWLEDGMENT

The authors would like to thank M. L. King from the University of Maryland and C. A. de Almeida from the National Institute for Space Research for all the support, and acknowledge the anonymous reviewers for the comments that helped improve the quality of this paper.

REFERENCES

[1] F. Achard *et al.*, "Determination of deforestation rates of the world's humid tropical forests," *Science*, vol. 297, pp. 999–1002, Aug. 9, 2002.
[2] M. C. Hansen *et al.*, "High-resolution global maps of 21st-century forest cover change," *Science*, vol. 342, pp. 850–853, Nov. 15, 2013.
[3] P. M. Fearnside, "The roles and movements of actors in the deforestation of Brazilian amazonia," *Ecol. Soc.*, vol. 13, no. 1, p. 23, 2008 [Online]. Available: http://www.ecologyandsociety.org/vol13/iss1/art23/
[4] J. A. Foley *et al.*, "Amazonia revealed: Forest degradation and loss of ecosystem goods and services in the Amazon Basin," *Front. Ecol. Environ.*, vol. 5, pp. 25–32, Feb. 1, 2007.
[5] D. S. Alves, "Space-time dynamics of deforestation in Brazilian Amazônia," *Int. J. Remote Sens.*, vol. 23, pp. 2903–2908, 2002.
[6] INPE, *Monitoramento da cobertura florestal da amazônia por satélites—sistemas prodes, deter, degrad e queimadas*. São Paulo, Brazil: INPE, 2008.
[7] A. C. Coutinho, C. Almeida, A. Venturieri, J. C. D. M. Esquerdo, and M. Silva, *Uso e cobertura da terra nas áreas desflorestadas da Amazônia Legal TerraClass 2008*. Brasília, Brazil: Embrapa, 2013.
[8] Y. E. Shimabukuro, G. T. Batista, E. M. K. Mello, J. C. Moreira, and V. Duarte, "Using shade fraction image segmentation to evaluate deforestation in Landsat Thematic Mapper images of the Amazon Region," *Int. J. Remote Sens.*, vol. 19, pp. 535–541, 1998.
[9] Brasil, "Plano Nacional sobre Mudança do Clima," ed. Brasilia, 2008, p. 154.
[10] IPEA, GIZ, and CEPAL, "Avaliação do plano de ação para prevenção e controle do desmatamento na amazônia legal—PPCDAM," 2011, p. 54.
[11] L. O. Anderson, Y. E. Shimabukuro, R. S. DeFries, and D. Morton, "Assessment of deforestation in near real time over the Brazilian Amazon using multitemporal fraction images derived from Terra MODIS," *IEEE Geosci. Remote Sens. Lett.*, vol. 2, no. 3, pp. 315–318, Jul. 2005.
[12] I. M. D. Rosa, C. Souza, and R. M. Ewers, "Changes in size of deforested patches in the Brazilian Amazon," *Conserv. Biol.*, vol. 26, pp. 932–937, 2012.
[13] M. I. S. Escada, L. E. Maurano, C. D. Rennó, S. Amaral, and D. M. Valeriano, "Avaliação de dados dos Sistemas de Alerta da Amazônia: DETER e SAD.," in *Proc. Simpósio Brasileiro de Sensoriamento Remoto*, Curitiba, Brazil, 2011, pp. 2934–2943.
[14] G. Gutman, C. Huang, G. Chander, P. Noojipady, and J. G. Masek, "Assessment of the NASA–USGS Global Land Survey (GLS) datasets," *Remote Sens. Environ.*, vol. 134, pp. 249–265, 2013.
[15] C. J. Tucker, D. M. Grant, and J. D. Dykstra, "NASA's global orthorectified Landsat data set," *Photogramm. Eng. Remote Sens.*, vol. 70, pp. 313–322, 2004.
[16] G. Câmara *et al.*, "TerraLib: An open source GIS library for large-scale environmental and socio-economic applications," in *Open Source Approaches in Spatial Data Handling*, vol. 2, G. B. Hall, M. Leahy, Eds. New York, NY, USA: Springer, 2008, pp. 247–270.
[17] Y. E. Shimabukuro and J. A. Smith, "The least-squares mixing models to generate fraction images derived from remote sensing multispectral data," *IEEE Trans. Geosci. Remote Sens.*, vol. 29, no. 1, pp. 16–20, Jan. 1991.
[18] G. P. Asner, C. E. Borghi, and R. A. Ojeda, *Desertification in Central Argentina: Changes in Ecosystem Carbon and Nitrogen From Imaging Spectroscopy*, vol. 13, Washington, DC, USA: Ecological Society of America, 2003.
[19] F. D. B. Espírito-Santo, Y. E. Shimabukuro, and T. M. Kuplich, "Mapping forest successional stages following deforestation in Brazilian Amazonia using multi-temporal Landsat images," *Int. J. Remote Sens.*, vol. 26, pp. 635–642, 2005.
[20] G. P. Asner, D. E. Knapp, E. N. Broadbent, P. J. C. Oliveira, M. Keller, and J. N. Silva, "Ecology: Selective logging in the Brazilian Amazon," *Science*, vol. 310, pp. 480–482, 2005.
[21] A. Alencar, G. P. Asner, D. Knapp, and D. Zarin, "Temporal variability of forest fires in eastern Amazonia," *Ecol. Appl.*, vol. 21, pp. 2397–2412, Oct. 1, 2011.
[22] E. S. Abreu, L. M. G. Fonseca, C. P. F. d. Santos, and V. O. Ribeiro, "'Cloud detection tool'—Uma ferramenta para a detecção de nuvens e sombras em imagens de satélite," in *Proc. Simpósio Brasileiro de Sensoriamento Remoto*, Foz do Iguaçu, Brasil, 2013, pp. 4234–4241.
[23] D. R. V. Moraes *et al.*, "Semi-automatic detection of cloud and shadows in the images of AWIFS sensor using the tool cloud detection," presented at the Latin Amer. Remote Sens. Week (LARS), Santiago, Chile, 2013.
[24] J. Gerwing and E. Vidal, *Degradação de Florestas pela Exploração Madeireira e Fogo na Amazônia Belém*. Belém, Brazil: Imazon, 2002.
[25] B. W. Nelson, V. Kapos, J. B. Adams, W. J. Oliveira, and O. P. G. Braun, "Forest disturbance by large blowdowns in the Brazilian Amazon," *Ecology*, vol. 75, pp. 853–858, Apr. 1, 1994.
[26] S. N. Goward *et al.*, "Complementarity of resourcesat-1 AWiFS and Landsat TM/ETM+ sensors," *Remote Sens. Environ.*, vol. 123, pp. 41–56, Aug. 2012.
[27] D. C. Morton, R. S. Defries, J. T. Randerson, L. Giglio, W. Schroeder, and G. R. Van Der Werf, "Agricultural intensification increases deforestation fire activity in Amazonia," *Global Change Biol.*, vol. 14, pp. 2262–2275, 2008.
[28] D. C. Morton *et al.*, "Cropland expansion changes deforestation dynamics in the southern Brazilian Amazon," *Proc. Nat. Acad. Sci. U.S.A.*, vol. 103, pp. 14637–14641, Sep. 2006.
[29] E. Barona, N. Ramankutty, G. Hyman, and O. T. Coomes, "The role of pasture and soybean in deforestation of the Brazilian Amazon," *Environ. Res. Lett.*, vol. 5, p. 024002, 2010.
[30] A. Lima *et al.*, "Land use and land cover changes determine the spatial relationship between fire and deforestation in the Brazilian Amazon," *Appl. Geogr.*, vol. 34, pp. 239–246, 2012.
[31] A. G. O. P. Barretto, G. Berndes, G. Sparovek, and S. Wirsenius, "Agricultural intensification in Brazil and its effects on land-use patterns: An analysis of the 1975–2006 period," *Global Change Biol.*, vol. 19, pp. 1804–1815, 2013.

[32] S. A. Spera *et al.*, "Recent cropping frequency, expansion, and abandonment in Mato Grosso, Brazil had selective land characteristics," *Environ. Res. Lett.*, vol. 9, p. 064010, 2014.
[33] J. Sun, Z. Huang, Q. Zhen, J. Southworth, and S. Perz, "Fractally deforested landscape: Pattern and process in a tri-national Amazon frontier," *Appl. Geogr.*, vol. 52, pp. 204–211, Aug. 2014.
[34] R. Verburg, S. R. Filho, D. Lindoso, N. Debortoli, G. Litre, and M. Bursztyn, "The impact of commodity price and conservation policy scenarios on deforestation and agricultural land use in a frontier area within the Amazon," *Land Use Policy*, vol. 37, pp. 14–26, Mar. 2014.
[35] M. A. Cochrane *et al.*, "Positive feedbacks in the fire dynamic of closed canopy tropical forests," *Science*, vol. 284, pp. 1832–1835, Jun. 11, 1999.
[36] D. C. Morton, Y. Le Page, R. DeFries, G. J. Collatz, and G. C. Hurtt, "Understorey fire frequency and the fate of burned forests in southern Amazonia," *Philos. Trans. Roy. Soc. B Biol. Sci.*, vol. 368, Jun. 5, 2013, doi: 10.1098/rstb.2012.0163.
[37] J. K. Balch, T. J. Massad, P. M. Brando, D. C. Nepstad, and L. M. Curran, "Effects of high-frequency understorey fires on woody plant regeneration in southeastern Amazonian forests," *Philos. Trans. Roy. Soc. B Biol. Sci.*, vol. 368, Jun. 5, 2013, doi: 10.1098/rstb.2012.0157.
[38] A. L. Silva Monteiro, P. G. Barreto, F. L. D. S. Pantoja, and J. J. Gerwing, "Impactos da exploração madeireira e do fogo em florestas de transição da Amazônia Legal," *Scientia Forestalis*, vol. 65, pp. 11–21, 2004.
[39] E. A. T. Matricardi, D. L. Skole, M. A. Pedlowski, and W. Chomentowski, "Assessment of forest disturbances by selective logging and forest fires in the Brazilian Amazon using Landsat data," *Int. J. Remote Sens.*, vol. 34, pp. 1057–1086, Feb. 20, 2013.
[40] E. A. T. Matricardi, D. L. Skole, M. A. Pedlowski, W. Chomentowski, and L. C. Fernandes, "Assessment of tropical forest degradation by selective logging and fire using Landsat imagery," *Remote Sens. Environ.*, vol. 114, pp. 1117–1129, May 17, 2010.
[41] P. Amaral, A. Veríssimo, P. Barreto, and E. Vidal, *Floresta para Sempre: um Manual para Produção de Madeira na Amazônia*. Belém, Brazil: Imazon, 1998.
[42] C. G. Diniz, J. S. Maia, A. A. A. Souza, D. C. Santos, M. C. Dias, and A. R. Gomes, "DETER AWIFS: Near real time deforestation detection," in *Proc. Latin Amer. Remote Sens. Week*, Santiago, Chile, 2013, pp. 15–19.
[43] D. C. Santos, D. M. C., A. A. A. Souza, C. G. Diniz, M. Adami, J. S. Maia *et al.*, "Identification and mapping of forest degradation patterns on the Brazilian Amazon based on AWIFS sensor image," in *Proc. Latin Amer. Remote Sens. Week*, Santiago, Chile, 2013, pp. 27–31.

Cesar Guerreiro Diniz was born in Belem, Brazil, in 1985. He received the B.S. degree in oceanography and the M.S. degree in geology from the Federal University of Para, Belem, Brazil, in 2009 and 2011, respectively.

He is currently with the Regional Center of the Amazon, National Institute for Space Research—INPE-CRA, Belem, Brazil.

Arleson Antonio de Almeida Souza was born in Belem, Brazil, in 1982. He received the B.S. degree in geography from the Federal University of Para, Belem, Brazil, in 2008. He is currently pursuing the M.S. degree in environmental science at Para State University, Belem, Brazil.

He is currently with the Regional Center of the Amazon, National Institute for Space Research—INPE-CRA, Belem, Brazil.

Diogo Corrêa Santos was born in Santos, Brazil, in 1984. He received the B.S. and M.S. degrees in geology from the Federal University of Para, Belem, Brazil, in 2009 and 2011, respectively.

He is currently with the Regional Center of the Amazon, National Institute for Space Research—INPE-CRA, Belem, Brazil.

Mirian Correa Dias was born in Belem, Brazil, in 1986. She received the B.S. degree in geography from the Federal University of Para, Belem, Brazil, in 2012. She is currently pursuing the M.S. degree in management of natural resources and local development in the Amazon at Federal University of Para, Belem, Brazil.

She is currently with the Regional Center of the Amazon, National Institute for Space Research—INPE-CRA, Belem, Brazil.

Nelton Cavalcante da Luz was born in Canarana, Brazil, in 1983. He received the B.S. degree in biology from the State University of Mato Grosso, Mato Grosso, Brazil, in 2008 and the M.S. degree in management of natural resources and local development in the Amazon from the Federal University of Para, Belem, Brazil, in 2011.

He is currently with the Regional Center of the Amazon, National Institute for Space Research—INPE-CRA, Belem, Brazil.

Douglas Rafael Vidal de Moraes was born in Belem, Brazil, in 1992. He received the B.S. degree in information systems from the Rural University of Para, Belem, Brazil, in 2015.

He is currently with the Regional Center of the Amazon, National Institute for Space Research—INPE-CRA, Belem, Brazil, as Fellow from the National Counsel of Technological and Scientific Development—CNPq, Brasília, Brazil.

Janaina Sant'Ana Maia was born in Taubaté, Brazil, in 1976. She received the M.S. degree in remote sensing from the National Institute for Space Research, Sao Jose dos Campos, Brazil, in 2002 and the Ph.D. degree in environmental engineering from the Federal University of Santa Catarina, Florianópolis, Brazil, in 2009.

She is currently with the Regional Center of the Amazon, National Institute for Space Research—INPE-CRA.

Alessandra Rodrigues Gomes was born in Campo Grande, Brazil, in 1974. She received the M.S. degree in remote sensing from the National Institute for Space Research, Sao Jose dos Campos, Brazil, in 2000 and the Ph.D. degree in geoscience from São Paulo State University, Rio Claro, Brazil, in 2011.

She is currently the Head of the Regional Center of the Amazon, National Institute for Space Research—INPE-CRA.

Igor da Silva Narvaes was born in Alegrete, Brazil, in 1976. He received the M.S. degree in forestry engineering from the Federal University of Santa Maria, Santa Maria, Brazil, in 2004 and the Ph.D. degree in remote sensing from the National Institute for Space Research, Sao Jose dos Campos, Brazil, in 2010.

He is currently with the INPE-CRA.

Dalton M. Valeriano was born in Juiz de Fora, Brazil, in 1956. He received the M.S. degree in remote sensing from the National Institute for Space Research, Belem, Brazil, in 1984 and the Ph.D. degree in geography from the University of California, Santa Barbara, CA, USA, in 1996.

He is currently with the National Institute for Space Research—INPE.

Luis Eduardo Pinheiro Maurano was born in Sao Paulo, Brazil, in 1965. He received the B.S. degree in computer science from the University Mackenzie of Sao Paulo, Sao Paulo, Brazil, in 1988.

He is currently with the National Institute for Space Research—INPE.

Marcos Adami was born in Machadinho, Brazil, in 1973. He received the M.S. and Ph.D. degrees in remote sensing from the National Institute for Space Research, Sao Jose dos Campos, Brazil, in 2003 and 2010, respectively.

He is currently with the INPE-CRA, Belem, Brazil.

View publication stats